- Tightening or loosening a pH-sensitive double-lasso molecular machine readily synthesized from an ends-activated [c2]daisy chain
  Romuald, C.; Ardá, A.; Clavel, C.; Barbero, J. J.; Coutrot, F. *Chem. Sci.* **2012**, *3*, 1851-1857.
  Abstract:

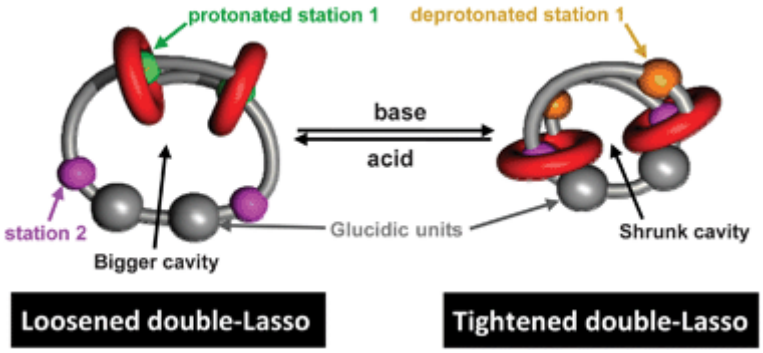

A solvent's polarity and pH variation triggers a jump rope movement and loosening or tightening of a double-lasso molecular machine.

- Poly(disulfide)s
  Bang, E. K.; Lista, M.; Sforazzini, G.; Sakai, N.; Matile, S. *Chem. Sci*. **2012**, *3*, 1752-1763.
  Abstract:

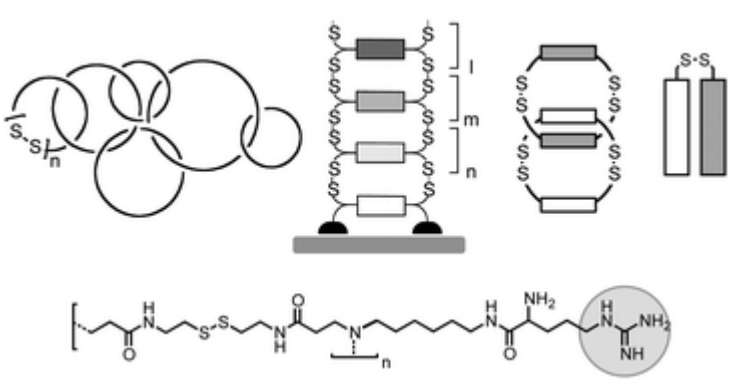

Recent progress with poly(disulfide)s is summarized comprehensively; highlights include dynamic topological plasticity, single-molecule detection methods, artificial photosystems as well as much excitement about gene delivery.

- Dual-Mode Control of PET Process in a Ferrocene-Functionalized [2]Rotaxane with High-Contrast Fluorescence Output
  Zhang, H.; Hu, J.; Qu, D.-H. *Org. Lett.* **2012**, *14*, 2334-2337.
  Abstract:

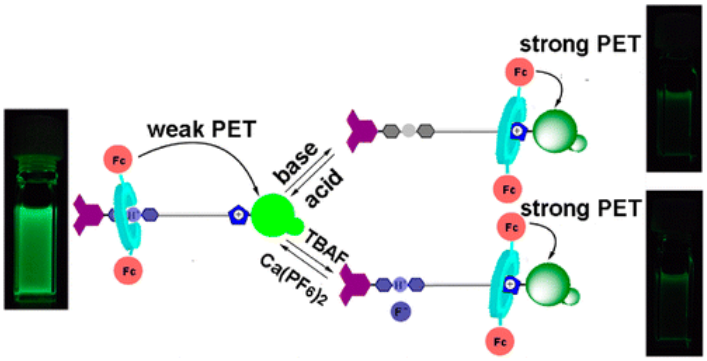

The shuttling motion of the ferrocene-functionalized macrocycle between the dibenzylammonium and the *N*-methyltriazolium recognition sites in a bistable [2]rotaxane, as well as the photoinduced electron transfer process occurring between ferrocene units and the morpholin-naphthalimide fluorescent stopper, can be adjusted not only by acid–base stimuli but also addition–removal of the fluoride anion, along with remarkable, high-contrast fluorescent intensity changes.

- Selective Synthesis of a [3]Rotaxane Consisting of Size-Complementary Components and Its Stepwise Deslippage
  Akae, Y.; Okamura, H.; Koyama, Y.; Arai, T.; Takata, T. *Org. Lett.* **2012**, *14*, 2226-2229.
  Abstract:

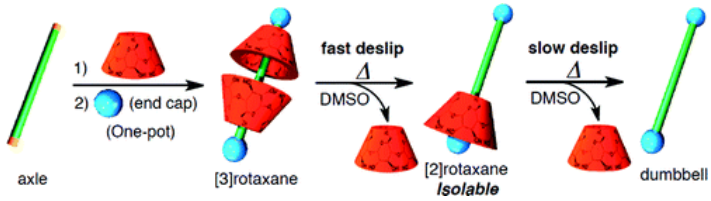

An α-cyclodextrin-based size-complementary [3]rotaxane with an alkylene axle was selectively synthesized in one pot via an end-capping reaction with 2-bromophenyl isocyanate in water. Thermal degradation of the [3]rotaxane product yielded not only the original components but also the [2]rotaxane. Thermodynamic studies suggested a stepwise deslippage process.

- Friedel–Crafts Acylation on Graphene
  Chua, C. K.; Pumera, M. *Chem. Asian J.* **2012**, *7*, 1009–1012.
  Abstract:

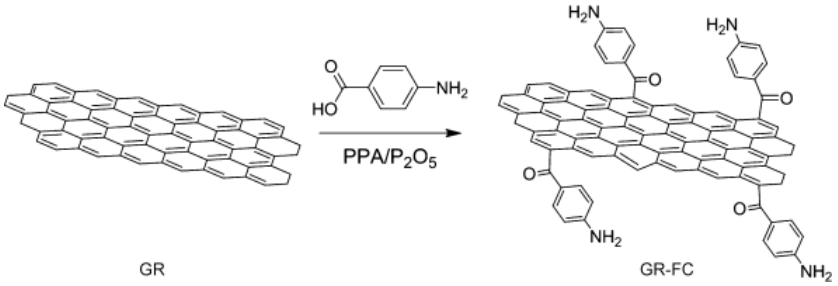

There is an excitement around graphene as a promising new material for nanotechnological and nanoarchitectonic applications. Despite the low chemical reactivity of graphene, chemical functionalization remains a prominent and viable solution to tailor its chemical, physical, and electronic properties. Herein, we report the covalent functionalization of reduced graphene oxide through Friedel–Crafts reactions under mild conditions of polyphosphoric-acid/phosphorus-pentoxide and 4-aminobenzoic acid. Successful functionalization was confirmed by X-ray photoelectron spectroscopy (XPS), FTIR, and Raman spectroscopy. The success of the Friedel–Crafts reaction provides an important expansion of the synthetic “toolbox” for future modifications of graphene towards the specific needs of different applications.

- Chemistry of Anthracene–Acetylene Oligomers XX: Synthesis, Structures, and Self-Association of Anthracene–Anthraquinone Cyclic Compounds with Ethynylene Linkers
  Iwanaga, T.; Miyamoto, K.; Tahara, K.; Inukai, K.; Okuhata, S.; Tobe, Y.; Toyota, S. *Chem. Asian J.* **2012**, *7*, 935–943.
  Abstract:

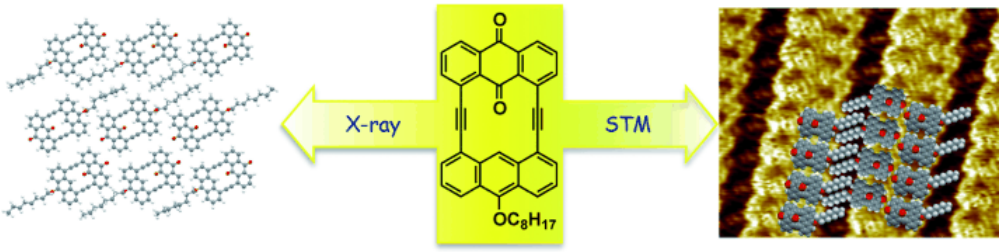

We have synthesized anthracene–acetylene oligomers, which contained one 10-substituted anthracene unit and one anthraquinone unit, by cyclization with Sonogashira coupling. X-ray analysis revealed an almost-planar framework and significant out-of-plane deformation around the inner carbonyl moiety because of steric hindrance. These compounds underwent self-association in solution and their association constants for monomer–dimer exchange were determined by variable-concentration ^{1}H NMR measurements in $CDCl_3$: 8 mol^{-1} L (10-substituent: isopropyl), <5 mol^{-1} L (methoxy), and 19 mol^{-1} L (octyloxy). These results were discussed on the basis of spectroscopic and molecular-orbital analysis. A linear molecular assembly of the octyloxy compound at a liquid/graphite interface was observed by STM measurements.

- Multiple Topologies from Glycopolypeptide–Dendron Conjugate Self-Assembly: Nanorods, Micelles, and Organogels
  Pati, D.; Kalva, N.; Das, S.; Kumaraswamy, G.; Gupta, S. S.; Ambade, A. V. *J. Am. Chem. Soc.* **2012**, *134*, 7796–7802.
  Abstract:

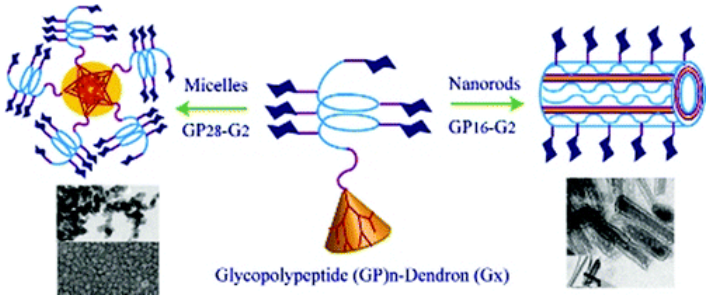

Glycopolypeptides (GPs) were synthesized by ring-opening polymerization of glycosylated *N*-carboxyanhydride monomer and attached to hydrophobic dendrons at one chain end by “click” reaction to obtain amphiphilic anisotropic macromolecules. We show that by varying polypeptide chain length and dendron generation, an organogel was obtained in dimethylsulfoxide, while nanorods and micellar aggregates were observed in aqueous solutions. Assemblies in water were characterized by electron microscopy and dye encapsulation. Secondary structure of the GP chain was shown to affect the morphology, whereas the chain length of the poly(ethylene glycol) linker between the GP and dendron did not alter rod-like assemblies. Bioactive surface chemistry of these assemblies displaying carbohydrate groups was demonstrated by interaction of mannose-functionalized nanorods with ConA.

- Supramolecularly Engineered Perylene Bisimide Assemblies Exhibiting Thermal Transition from Columnar to Multilamellar Structures
  Yagai, S.; Usui, M.; Seki, T.; Murayama, H.; Kikkawa, Y.; Uemura, S.; Karatsu, T.; Kitamura, A.; Asano, A.; Seki, S. *J. Am. Chem. Soc.* **2012**, *134*, 7983–7994.
  Abstract:

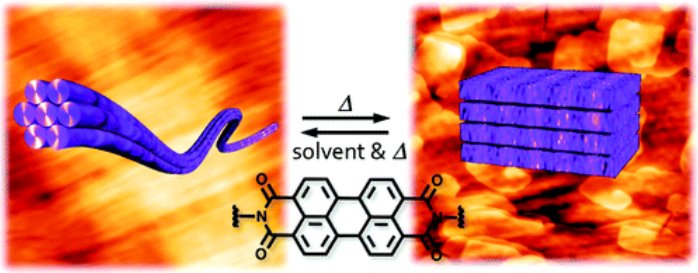

Perylene 3,4:9,10-tetracarboxylic acid bisimide (PBI) was functionalized with ditopic cyanuric acid to organize it into complex columnar architectures through the formation of hydrogen-bonded supermacrocycles (rosette) by complexing with ditopic melamines possessing solubilizing alkoxyphenyl substituents. The aggregation study in solution using UV–vis and NMR spectroscopies showed the formation of extended aggregates through hydrogen-bonding and π–π stacking interactions. The cylindrical fibrillar nanostructures were visualized by microscopic techniques (AFM, TEM), and the formation of lyotropic mesophase was confirmed by polarized optical microscopy and SEM. X-ray diffraction study revealed that a well-defined hexagonal columnar (Col_h) structure was formed by solution-casting of fibrillar assemblies. All of these results are consistent with the formation of hydrogen-bonded PBI rosettes that spontaneously organize into the Col_h structure. Upon heating the Col_h structure in the bulk state, a structural transition to a highly ordered lamellar (Lam) structure was observed by variable-temperature X-ray diffraction, differential scanning calorimetry, and AFM studies. IR study showed that the rearrangement of the hydrogen-bonding motifs occurs during the structural transition. These results suggest that such a striking structural transition is aided by the reorganization in the lowest level of self-organization, i.e., the rearrangement of hydrogen-bonded motifs from rosette to linear tape. A remarkable increase in the transient photoconductivity was observed by the flash-photolysis time-resolved microwave conductivity (FP-TRMC) measurements upon converting the Col_h structure to the Lam structure. Transient absorption spectroscopy revealed that electron transfer from electron-donating alkoxyphenyl groups of melamine components to electron-deficient PBI moieties takes place, resulting in a higher probability of charge carrier generation in the Lam structure compared to the Col_h structure.

- Site-Specific Mapping and Time-Resolved Monitoring of Lysine Methylation by High-Resolution NMR Spectroscopy
  Theillet, F.-X.; Liokatis, S.; Jost, J. O.; Bekei, B.; Rose, H. M.; Binolfi, A.; Schwarzer, D.; Selenko, P. *J. Am. Chem. Soc.* **2012**, *134*, 7616–7619.
  Abstract:

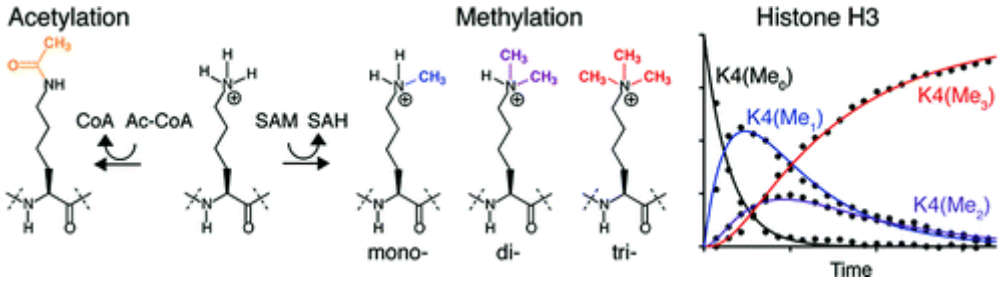

Methylation and acetylation of protein lysine residues constitute abundant post-translational modifications (PTMs) that regulate a plethora of biological processes. In eukaryotic proteins, lysines are often mono-, di-, or trimethylated, which may signal different biological outcomes.

Deconvoluting these different PTM types and PTM states is not easily accomplished with existing analytical tools. Here, we demonstrate the unique ability of NMR spectroscopy to discriminate between lysine acetylation and mono-, di-, or trimethylation in a site-specific and quantitative manner. This enables mapping and monitoring of lysine acetylation and methylation reactions in a nondisruptive and continuous fashion. Time-resolved NMR measurements of different methylation events in complex environments including cell extracts contribute to our understanding of how these PTMs are established *in vitro* and *in vivo*.

- Perylene-3-ylmethanol: Fluorescent Organic Nanoparticles as a Single-Component Photoresponsive Nanocarrier with Real-Time Monitoring of Anticancer Drug Release
  Jana, A.; Devi, K. S. P.; Maiti, T. K.; Singh, N. D. P. *J. Am. Chem. Soc.* **2012**, *134*, 7656–7659.
  Abstract:

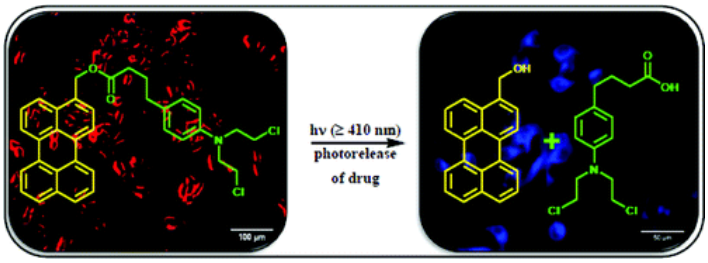

We report for the first time the use of perylene-3-ylmethanol fluorescent organic nanoparticles as a drug delivery system. In the present system, perylene-3-ylmethanol nanoparticles performed four important roles: (i) “nanocarriers” for drug delivery; (ii) “phototriggers” for the drug release; (iii) fluorescent chromophores for cell imaging; and (iv) detectors for real time-monitoring of drug release. In vitro biological studies revealed that the newly developed perylene-3-ylmethanol nanoparticles exhibit good biocompatibility and cellular uptake as well as efficient photoregulated anticancer drug release ability. Such fluorescent organic nanoparticles may open up new perspectives for designing a new class of promising photoresponsive nanocarriers for drug delivery.

- High-Transconductance Organic Thin-Film Electrochemical Transistors for Driving Low-Voltage Red-Green-Blue Active Matrix Organic Light-Emitting Devices
  Braga, D.; Erickson, N. C.; Renn, M. J.; Holmes, R. J.; Frisbie, C. D. *Adv. Funct. Mater.* **2012**, *22*, 1623–1631.
  Abstract:

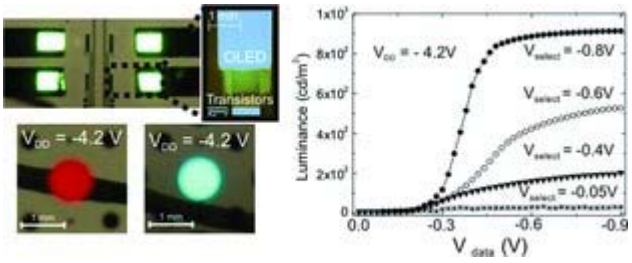

Switching and control of efficient red, green, and blue active matrix organic light-emitting devices (AMOLEDs) by printed organic thin-film electrochemical transistors (OETs) are demonstrated. These all-organic pixels are characterized by high luminance at low operating voltages and by extremely small transistor dimensions with respect to the OLED active area. A maximum brightness of ≈900 cd m^{-2} is achieved at diode supply voltages near 4 V and pixel selector (gate) voltages below 1 V. The ratio of OLED to OET area is greater than 100:1 and the pixels may be switched at rates up to 100 Hz.

Essential to this demonstration are the use of a high capacitance electrolyte as the gate dielectric layer in the OETs, which affords extremely large transistor transconductances, and novel graded emissive layer (G-EML) OLED architectures that exhibit low turn-on voltages and high luminescence efficiency. Collectively, these results suggest that printed OETs, combined with efficient, low voltage OLEDs, could be employed in the fabrication of flexible full-color AMOLED displays.

- High-Performance Metal-Free Solar Cells Using Stamp Transfer Printed Vapor Phase Polymerized Poly(3,4-Ethylenedioxythiophene) Top Anodes
  Wang, X.; Ishwara, T.; Gong, W.; Campoy-Quiles, M.; Nelson, J.; Bradley, D. D. C. *Adv. Funct. Mater.* **2012**, *22*, 1454–1460.
  Abstract:

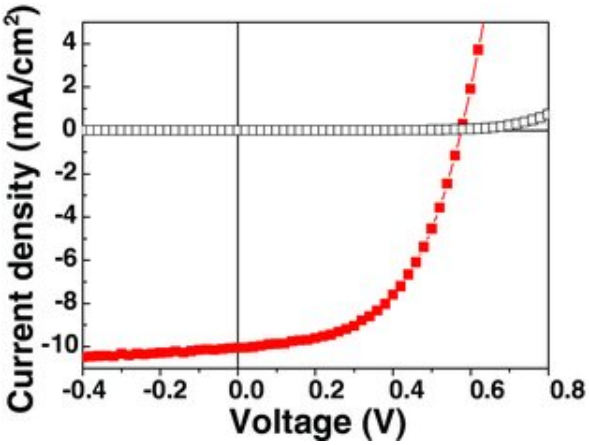

The use of vapor phase polymerized poly(3,4-ethylenedioxythiophene) (VPP-PEDOT) as a metal-replacement top anode for inverted solar cells is reported. Devices with both i) standard bulk heterojunction blends of poly(3-hexylthiophene) (P3HT) donor and 1-(3-methoxycarbonyl)-propyl-1-phenyl-(6,6)C_{60} (PCBM) soluble fullerene acceptor and ii) hybrid inorganic/organic TiO_2/P3HT acceptor/donor active layers are studied. Stamp transfer printing methods are used to deposit both the VPP-PEDOT top anode and a work function enhancing PEDOT:polystyrenesulphonate (PEDOT:PSS) interlayer. The metal-free devices perform comparably to conventional devices with an evaporated metal top anode, yielding power conversion efficiencies of 3% for bulk heterojunction blend and 0.6% for organic/inorganic hybrid structures. These encouraging results suggest that stamp transfer printed VPP-PEDOT provides a useful addition to the electrode materials tool-box available for low temperature and non-vacuum solar cell fabrication.

- Resettable Fluorescence Logic Gate Based on Calcein/Layered Double Hydroxide Ultrathin Films
  Shi, W.; Ji, X.; Wei, M.; Evans, D. G.; Duan, X. *Langmuir* **2012**, *28*, 7119-7124.
  Abstract:

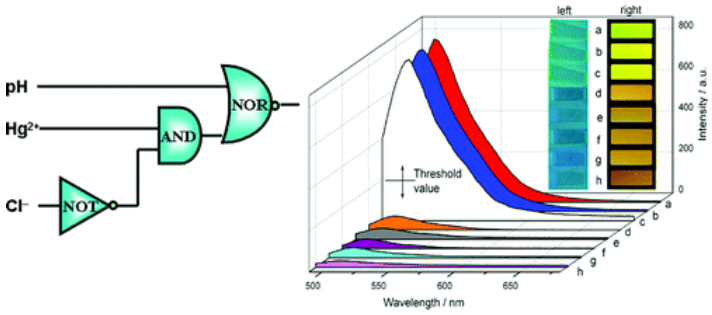

A fluorescent logic gate was fabricated based on calcein/layered double hydroxide ultrathin films (UTFs) via alternate assembly technique, which exhibits high stability, reversibility, and resettability. The logic gate was manipulated by utilizing pH value, Hg^{2+} and Cl^- ion as inputs, and the fluorescence emission of the $(calcein/LDH)_{16}$ UTF as output, serving as a three-input logic gate that combines the YES and INHIBIT operation.

- Flexible Transparent PES/Silver Nanowires/PET Sandwich-Structured Film for High-Efficiency Electromagnetic Interference Shielding
  Hu, M.; Gao, J.; Dong, Y.; Li, K.; Shan, G.; Yang, S.; Li, R. K.-Y. *Langmuir* **2012**, *28*, 7101-7106.
  Abstract:

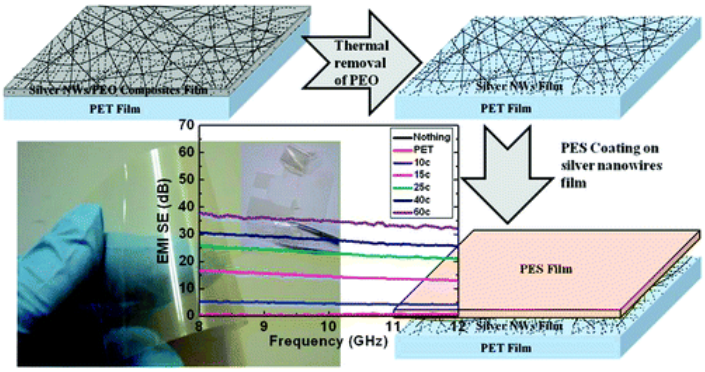

We have developed a kind of high-yield synthesis strategy for silver nanowires by a two-step injection polyol method. Silver nanowires and polyethylene oxide (PEO) (M_w = 900 000) were prepared in a homogeneous-coating ink. Wet composite films with different thicknesses were fabricated on a PET substrate by drawn-down rod-coating technology. Silver nanowires on PET substrates present a homogeneous distribution under the assistance of PEO. Then PEO was thermally removed in situ at a relatively low temperature attributed to its special thermal behavior under atmospheric conditions. As-prepared metallic nanowire films on PET substrates show excellent stability and a good combination of conductivity and light transmission. A layer of transparent poly(ethersulfones) (PESs) was further coated on silver nanowire networks by the same coating method to prevent the shedding and corrosion of silver nanowires. Sandwich-structured flexible transparent films were obtained and displayed excellent electromagnetic interference (EMI) shielding effectiveness.

- Modeling the Crystallization of Spherical Nucleic Acid Nanoparticle Conjugates with Molecular Dynamics Simulations
  Li, T. I. N. G.; Sknepnek, R.; Macfarlane, R. J.; Mirkin, C. A.; de la Cruz, M. O. *Nano Letters* **2012**, *12*, 2509-2514.
  Abstract:

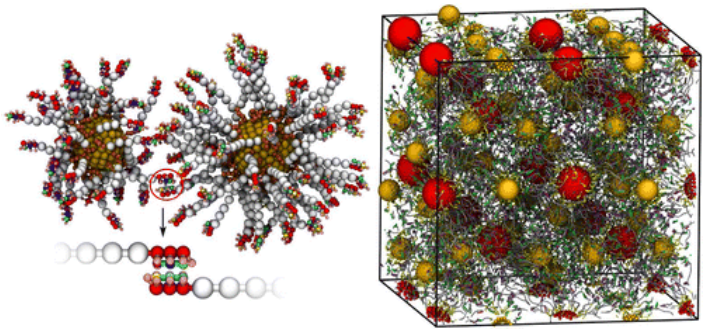

We use molecular dynamics simulations to study the crystallization of spherical nucleic-acid (SNA) gold nanoparticle conjugates, guided by sequence-specific DNA hybridization events. Binary mixtures of SNA gold nanoparticle conjugates (inorganic core diameter in the 8–15 nm range) are shown to assemble into BCC, CsCl, AlB_2, and Cr_3Si crystalline structures, depending upon particle stoichiometry, number of immobilized strands of DNA per particle, DNA sequence length, and hydrodynamic size ratio of the conjugates involved in crystallization. These data have been used to construct phase diagrams that are in excellent agreement with experimental data from wet-laboratory studies.

- Low-Temperature Preparation of Tailored Carbon Nanostructures in Water
  Szilluweit, R.; Hoheisel, T. N.; Fritzsche, M.; Ketterer, B.; Fontcuberta i Morral, A.; Demurtas, D.; Laporte, V.; Verel, R.; Bolisetty, S.; Mezzenga, R.; Frauenrath, H. *Nano Letters* **2012**, *12*, 2573-2578.
  Abstract:

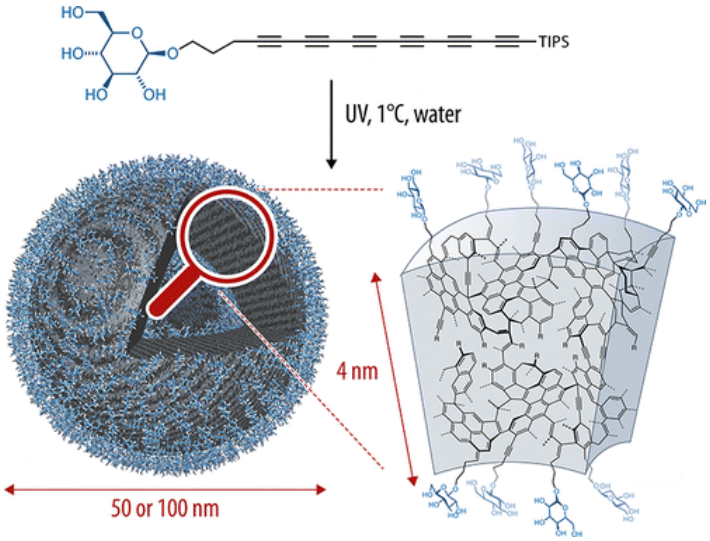

The development of low-temperature carbonization procedures promises to provide novel nanostructured carbon materials that are of high current interest in materials science and technology. Here, we report a “wet-chemical” carbonization method that utilizes hexayne amphiphiles as metastable carbon precursors. Nearly perfect control of the nanoscopic morphology was achieved by self-assembly of the precursors into colloidal aggregates with tailored diameter in water. Subsequent carbonization furnished carbon nanocapsules with a carbon microstructure resembling graphite-like amorphous carbon materials.

- Catalytic Janus Motors on Microfluidic Chip: Deterministic Motion for Targeted Cargo Delivery
  Baraban, L.; Makarov, D.; Streubel, R.; Mönch, I.; Grimm, D.; Sanchez, S.; Schmidt, O. G. *ACS Nano* **2012**, *6*, 3383-3389.
  Abstract:

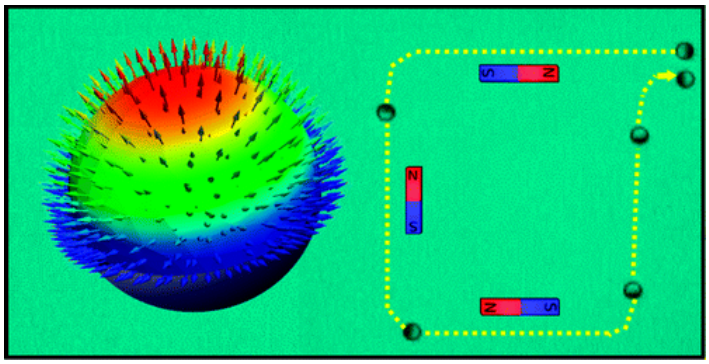

We fabricated self-powered colloidal Janus motors combining catalytic and magnetic cap structures, and demonstrated their performance for manipulation (uploading, transportation, delivery) and sorting of microobjects on microfluidic chips. The specific magnetic properties of the Janus motors are provided by ultrathin multilayer films that are designed to align the magnetic moment along the main symmetry axis of the cap. This unique property allows a deterministic motion of the Janus particles at a large scale when guided in an external magnetic field. The observed directional control of the motion combined with extensive functionality of the colloidal Janus motors conceptually opens a straightforward route for targeted delivery of species, which are relevant in the field of chemistry, biology, and medicine.

- Probing the stability of nonglycosylated wild-type erythropoietin protein via reiterative alanine ligations
  Brailsford, J. A.; Danishefsky, S. J. *Proc. Nat. Acad. Sci. USA* **2012**, *109*, 7196-7201.
  Abstract:

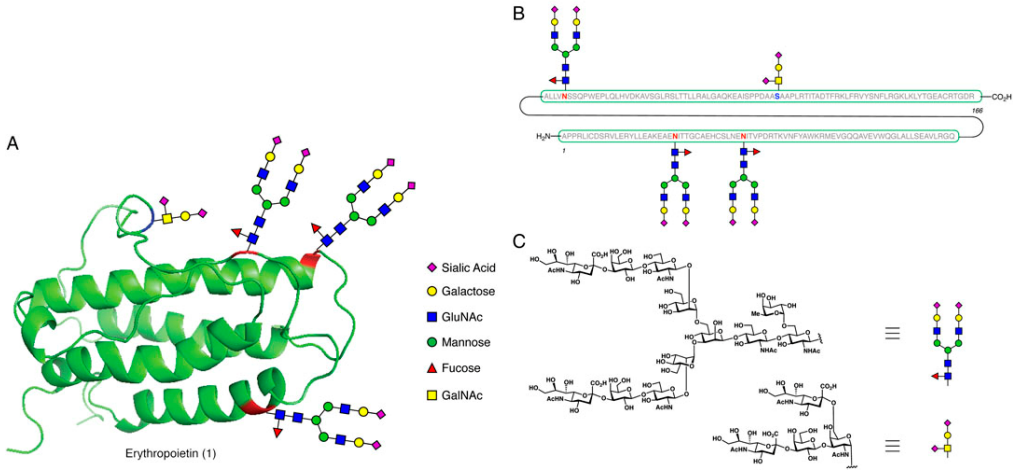

Nonglycosylated erythropoietin bearing acetamidomethyl protecting groups at the cysteine residues has been synthesized via chemical methods. Alanine ligation was used to assemble four peptide fragments, themselves prepared by solid phase peptide synthesis. This work outlines a route for the synthesis of homogeneous glycosylated erythropoietin.

- Histidine pairing at the metal transport site of mammalian ZnT transporters controls Zn^{2+} over Cd^{2+} selectivity
  Hoch, E.; Lin, W.; Chai, J.; Hershfinkel, M.; Fu, D.; Sekler, I. *Proc. Nat. Acad. Sci. USA* **2012**, *109*, 7202-7207.
  Abstract:

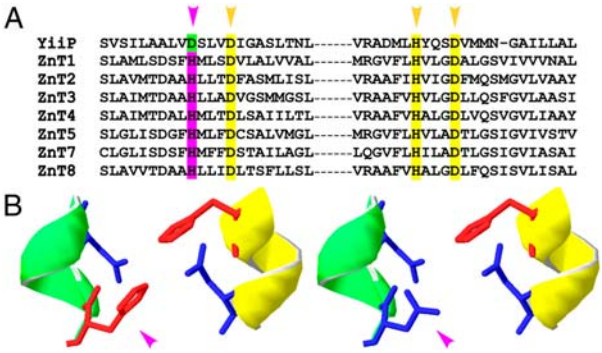

Zinc and cadmium are similar metal ions, but though Zn^{2+} is an essential nutrient, Cd^{2+} is a toxic and common pollutant linked to multiple disorders. Faster body turnover and ubiquitous distribution of Zn^{2+} vs. Cd^{2+} suggest that a mammalian metal transporter distinguishes between these metal ions. We show that the mammalian metal transporters, ZnTs, mediate cytosolic and vesicular Zn^{2+} transport, but reject Cd^{2+}, thus constituting the first mammalian metal transporter with a refined selectivity against Cd^{2+}. Remarkably, the bacterial ZnT ortholog, YiiP, does not discriminate between Zn^{2+} and Cd^{2+}. A phylogenetic comparison between the tetrahedral metal transport motif of YiiP and ZnTs identifies a histidine at the mammalian site that is critical for metal selectivity. Residue swapping at this position abolished metal selectivity of ZnTs, and fully reconstituted selective Zn^{2+} transport of YiiP. Finally, we show that metal selectivity evolves through a reduction in binding but not the translocation of Cd^{2+} by the transporter. Thus, our results identify a unique class of mammalian transporters and the structural motif required to discriminate between Zn^{2+} and Cd^{2+}, and show that metal selectivity is tuned by a coordination-based mechanism that raises the thermodynamic barrier to Cd^{2+} binding.

- Computational design of a protein crystal.
  Lanci, C. J.; MacDermaid, C. M.; Kang, S.; Acharya, R.; North, B.; Yang, X.; Qiu, X. J.; DeGrado, W. F.; Saven, J. G. *Proc. Nat. Acad. Sci. USA* **2012**, *109*, 7304-7309.
  Abstract:

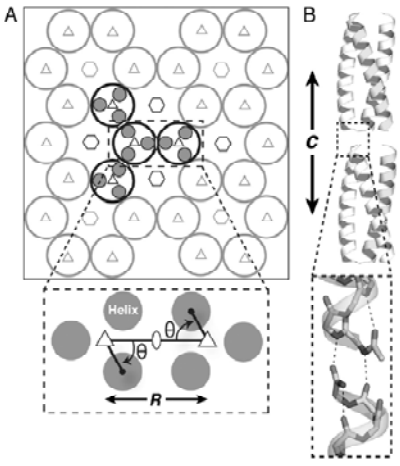

Protein crystals have catalytic and materials applications and are central to efforts in structural biology and therapeutic development. Designing predetermined crystal structures can be subtle given the complexity of proteins and the noncovalent interactions that govern crystallization. De novo protein design provides an approach to engineer highly complex nanoscale molecular structures, and often the positions of atoms can be programmed with sub-Å precision. Herein, a computational approach is presented for the design of proteins that self-assemble in three

dimensions to yield macroscopic crystals. A three-helix coiled-coil protein is designed de novo to form a polar, layered, three-dimensional crystal having the P6 space group, which has a “honeycomb-like” structure and hexameric channels that span the crystal. The approach involves: (i) creating an ensemble of crystalline structures consistent with the targeted symmetry; (ii) characterizing this ensemble to identify “designable” structures from minima in the sequencestructure energy landscape and designing sequences for these structures; (iii) experimentally characterizing candidate proteins. A 2.1 Å resolution X-ray crystal structure of one such designed protein exhibits sub-Å agreement [backbone root mean square deviation (rmsd)] with the computational model of the crystal. This approach to crystal design has potential applications to the de novo design of nanostructured materials and to the modification of natural proteins to facilitate X-ray crystallographic analysis.

- A Stem Cell-Based Approach to Cartilage Repair.
  Johnson, K.; Zhu, S.; Tremblay, M. S.; Payette, J. N.; Wang, J.; Bouchez, L. C.; Meeusen, S.; Althage, A.; Cho, C. Y.; Wu, X.; Schultz, P. G. *Science* **2012**, *336*, 717-721.
  Abstract:

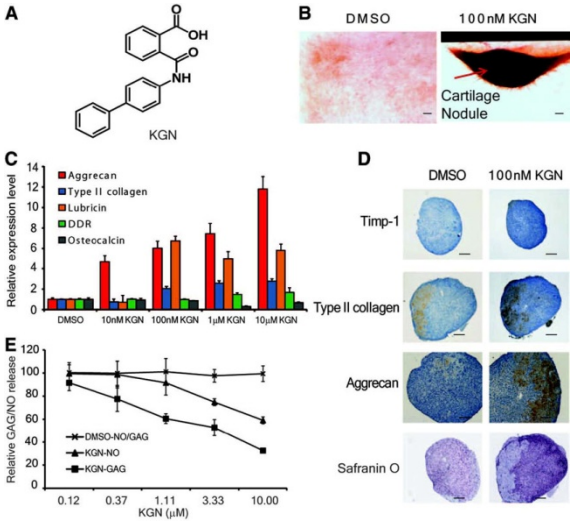

Osteoarthritis (OA) is a degenerative joint disease that involves the destruction of articular cartilage and eventually leads to disability. Molecules that promote the selective differentiation of multipotent mesenchymal stem cells (MSCs) into chondrocytes may stimulate the repair of damaged cartilage. Using an image-based high-throughput screen, we identified the small molecule kartogenin, which promotes chondrocyte differentiation (median effective concentration = 100 nM), shows chondroprotective effects in vitro, and is efficacious in two OA animal models. Kartogenin binds filamin A, disrupts its interaction with the transcription factor core-binding factor b subunit (CBFb), and induces chondrogenesis by regulating the CBFb-RUNX1 transcriptional program. This work provides new insights into the control of chondrogenesis that may ultimately lead to a stem cell-based therapy for osteoarthritis.

- Effect of o-Carborane on the Optoelectronic and Device-Level Properties of Poly(fluorene)s
  Davis, A. R.; Peterson, J. J.; Carter, K. R. *ACS Macro Lett.* **2012**, *1*, 469–472.
  Abstract:

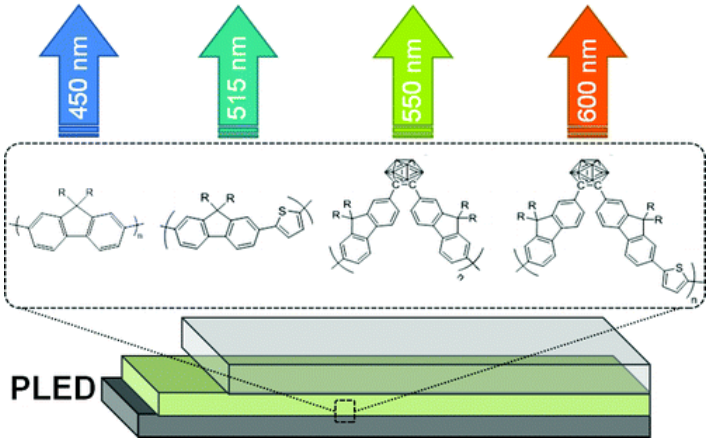

Carboranes have been previously noted to distinctively affect the luminescent properties of semiconducting polymers when incorporated into the conjugated backbone. In this report, we use carborane-based poly(fluorene) derivatives as active materials for polymer light-emitting diodes and transistors. Optoelectronic analysis unequivocally shows that carborane does not participate in the π-conjugated network, yet their presence causes major red-shifting in device electroluminescence as well as in thin film photoluminescence. In field effect transistors, they also improve charge carrier mobility by an order of magnitude despite disrupting π-conjugation. This use of carborane-containing conjugated polymers in active devices holds promise as new responsive materials in electronic polymer applications.

- Unimolecular Janus Micelles by Microenvironment-Induced, Internal Complexation
  Steinschulte, A. A.; Schulte, B.; Erberich, M.; Borisov, O. V.; Plamper, F. A. *ACS Macro Lett.* **2012**, *1*, 504–507.
  Abstract:

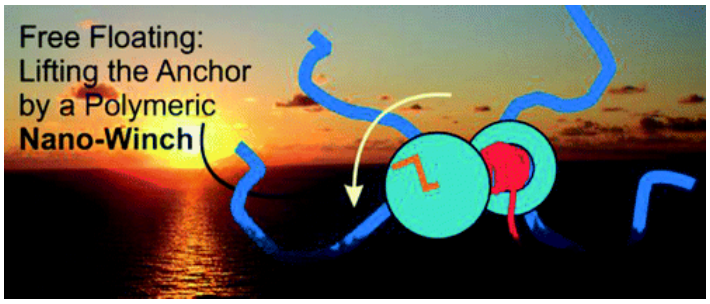

A noncentrosymmetric, star-shaped polymeric system is presented, which forms unimolecular micelles upon complexation of poly(propylene oxide) (PPO) with poly(dimethylaminoethyl methacrylate) (PDMAEMA). The influence of macromolecular architecture on the hydrophobicity of PPO and its interaction with PDMAEMA is investigated. Within stars, a complex between PPO and PDMAEMA is formed, lowering the interfacial tension of the hydrophobic domain (PDMAEMA acts as a “microsurfactant” for PPO). This leads to a pronounced drop in aggregation number compared to similar diblock copolymers, as corroborated by a scaling approach.

- Molecular Assembly Directed by Metal–Aromatic Interactions: Control of the Aggregation and Photophysical Properties of Zn–Salen Complexes by Aromatic Mercuration
  Cai, Y.-B.; Zhan, J.; Hai, Y.; Zhang, J.-L. *Chem. Eur. J.* **2012**, *18*, 4242 – 4249.
  Abstract:

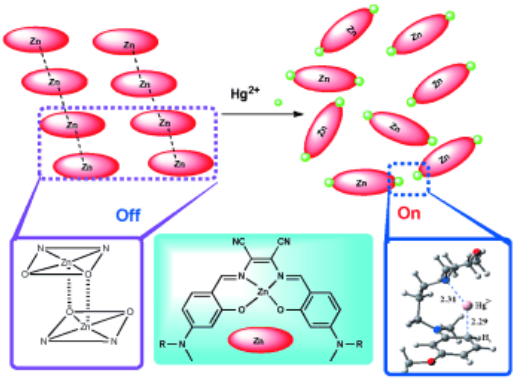

There is widespread interest in non-covalent bonding and weak interactions, such as electrostatic interactions, hydrogen bonding, solvophobic/hydrophobic interactions, metal–metal interactions, and π–π stacking, to tune the molecular assembly of planar π-conjugated organic and inorganic molecules. Inspired by the roles of metal–aromatic interaction in biological systems, such as in ion channels and metalloproteins, herein, we report the first example of the use of Hg^{2+}–aromatic interactions to selectively control the assembly and disassembly of zinc–salen complexes in aqueous media; moreover, this process exhibited significant "turn on" fluorescent properties. UV/Vis and fluorescence spectroscopic analysis of the titration of Hg^{2+} ions versus complex ZnL1 revealed that the higher binding affinity of Hg^{2+} ions (compared to 13 other metal ions) was ascribed to specific interactions between the Hg^{2+} ions and the phenyl rings of ZnL1; this result was also confirmed by 1H NMR spectroscopy and HRMS (ESI). Further evidence for this type of interaction was obtained from the reaction of small-molecule analogue L1with Hg^{2+} ions, which demonstrates the proximity of the *N*-alkyl group to the aromatic protons during Hg^{2+}-ion binding, which led to the consequential H/D exchange reaction with D_2O. DFT modeling of such interactions between the Hg^{2+} ions and the phenyl rings afforded calculated distances between the C and Hg atoms (2.29 Å) that were indicative of C-Hg bond-formation, under the direction of the N atom of the morpholine ring. The unusual coordination of Hg^{2+} ions to the phenyl ring of the metallosalen complexes not only strengthened the binding ability but also increased the steric effect to promote the disassembly of ZnL1 in aqueous media.

- A Supramolecular Polymer Blend Containing Two Different Supramolecular Polymers through Self-Sorting Organization of Two Heteroditopic Monomers
  Dong, S.; Yan, X.; Zheng, B.; Chen, J.; Ding, X.; Yu, Y.; Xu, D.; Zhang, M.; Huang, F. *Chem. Eur. J.* **2012**, *18*, 4195 – 4199.
  Abstract:

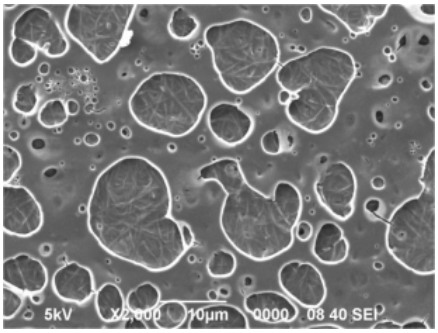

Sorting itself out: A novel and modular supramolecular polymer blend was prepared by means of self-sorting organization of two heteroditopic AB-type monomers. By blending two different low-molecular-weight molecules, versatile and interesting micro- and macroscopic aggregates were

prepared. This research provides a powerful strategy to prepare complex and highly ordered structures.

- Efficient Solid Emitters with Aggregation-Induced Emission and Intramolecular Charge Transfer Characteristics: Molecular Design, Synthesis, Photophysical Behaviors, and OLED Application
  Yuan, W. Z.; Gong, Y.; Chen, Y.; Shen, X. Y.; Lam, J. W. Y.; Lu, P.; Lu, Y.; Wang, Z.; Hu, R.; Xie, N.; Kwok, H. S.; Zhang, Y.; Sun, J. Z.; Tang, B. Z. *Chem. Mater.* **2012**, *24*, 1518–1528.
  Abstract:

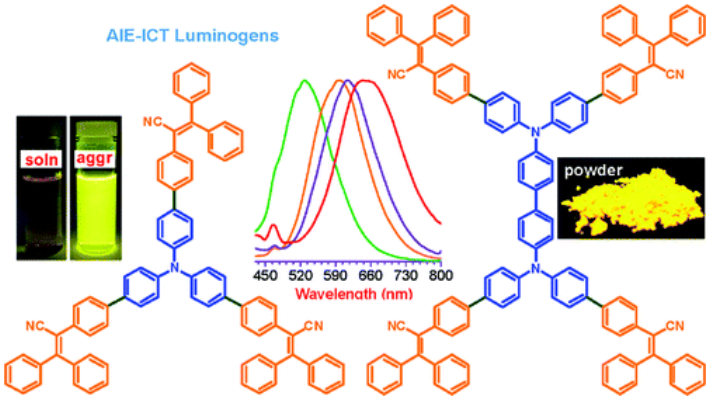

Emissive electron donor–acceptor (D–A) conjugates have a wide variety of applications in biophotonics, two-photon absorption materials, organic lasers, long wavelength emitters, and so forth. However, it is still a challenge to synthesize high solid-state efficiency D–A structured emitters due to the notorious aggregation-caused quenching (ACQ) effect. Though some D–A systems are reported to show aggregation-induced emission (AIE) behaviors, most are only selectively AIE-active in highly polar solvents, showing decreased solid-sate emission efficiencies compared to those in nonpolar solvents. Here we report the triphenylamine (TPA) and 2,3,3-triphenylacrylonitrile (TPAN) based D–A architectures, namely, TPA3TPAN and DTPA4TPAN. Decoration of arylamines with TPAN changes their emission behaviors from ACQ to AIE, making resulting TPA3TPAN and DTPA4TPAN nonluminescent in common solvents but highly emissive when aggregated as nanoparticles, solid powders, and thin films owing to their highly twisted configurations. Both compounds also display a bathochromic effect due to their intramolecular charge transfer (ICT) attribute. Combined ICT and AIE features render TPA3TPAN and DTPA4TPAN intense solid yellow emitters with quantum efficiencies of 33.2% and 38.2%, respectively. They are also thermally and morphologically stable, with decomposition and glass transition temperatures (T_d/T_g) being 365/127 and 377/141 °C, respectively. Multilayer electroluminescence (EL) devices are constructed, which emit yellow EL with maximum luminance, current, power, and external quantum efficiencies up to 3101 cd/m^2, 6.16 cd/A, 2.64 lm/W, and 2.18%, respectively. These results indicate that it is promising to fabricate high efficiency AIE-ICT luminogens with tunable emissions through rational combination and modulation of propeller-like donors and/or acceptors, thus paving the way for their biophotonic and optoelectronic applications.

- A *m*-Terphenyl-Modifed Sulfone Derivative as a Host Material for High-Efficiency Blue and Green Phosphorescent OLEDs
  Sasabe, H.; Seino, Y.; Kimura, M.; Kido, J. *Chem. Mater.* **2012**, *24*, 1404–1406.
  Abstract:

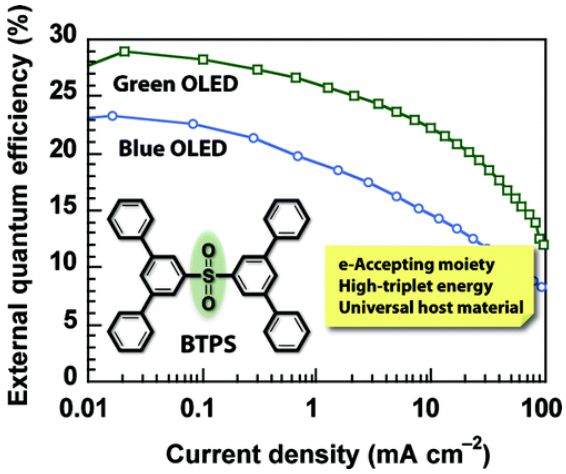

High-efficiency organic light-emitting devices (OLEDs) have received considerable attention for energy-saving solid-state lighting and eco-friendly flat panel display applications. For an energy-saving illumination light source beyond the fluorescent tube, the use of phosphorescent OLED technology is imperative because a phosphorescent emitter can yield an internal quantum efficiency as high as 100%. In phosphorescent OLEDs, a host material plays a key role in determining OLED performances. Among the known host materials, a host material with an electron-accepting moiety, such as pyridine, pyrimidine, and phosphine-oxide, can realize high performances in blue and green OLEDs. This type of host can promote electron injection as well as electron transport, creating an improved carrier balance of holes and electrons in an emissive layer (EML).

In this regard, a sulfone-containing material is an attractive candidate to present a great opportunity for a phosphorescent host material, because a sulfone moiety possesses a strong electron-accepting nature. Some sulfone-containing materials have been used as an emitter and an electron transporter to realize high-performance fluorescent OLEDs so far. On the other hand, Hsu and co-workers have reported triphenylamine/bisphenylsulfonyl-substituted fluorene material for red phosphorescent OLEDs. Most recently, Kim and co-workers have developed a solution-processed blue phosphorescent OLED with an external quantum efficiency (η_{ext}) of 6.9% and a current efficiency (η_c) of 12.9 cd A^{-1} at 100 cd m^{-2} using 4,4′-bis(phenylsulfonyl)biphenyl (SO1) and a common blue phosphorescent emitter iridium(III) bis[(4,6-difluorophenyl)-pyridinate-*N*,$C^{2'}$]picolinate (FIrpic). Even though sulfone-containing derivatives can hold tremendous promises as a host material in phosphorescent OLEDs, their performances are limited and the full potential is yet to be explored. We have already reported that *m*-terphenyl-modified carbazole derivative (CzTP) has a high thermal stability and a triplet energy (E_T) of 2.70 eV to realize high-performance blue and green OLEDs. In this communication, we introduce a *m*-terphenyl-modified sulfone derivative, 5′,5′′′′-sulfonyl-di-1,1′:3′,1″-terphenyl (BTPS, Figure 1) as a host material for phosphorescent blue and green OLEDs.

- Oligopyrenotides: Chiral Nanoscale Templates for Chromophore Assembly
  Malinovskii, V. L.; Nussbaumer, A. L.; Häner, R. *Angew. Chem. Int. Ed.* **2012**, *51*, 4905-4908.
  Abstract:

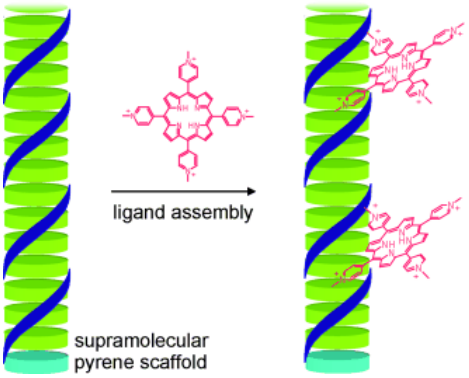

Getting organized: DNA-like supramolecular polymers formed of short oligopyrenotides serve as a helical scaffold for the molecular assembly of ligands (see picture). The cationic porphyrin meso-tetrakis(1-methylpyridin-4-yl)porphyrin interacts with the helical polymers in a similar way as with poly(dA:dT).

- Azobenzenes in a New Light—Switching In Vivo
  Wegner, H. A. *Angew. Chem. Int. Ed.* **2012**, *51*, 4787-4788.
  Abstract:

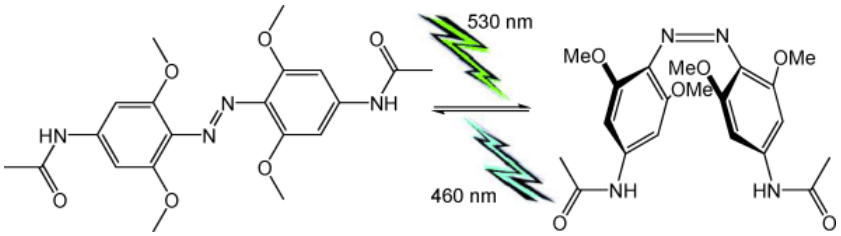

Two bands make light work: Since the isomerization of azobenzenes is usually induced by UV light, its application is limited in living systems. A new azobenzene switch now operates entirely in the visible range. The new design is based on the introduction of OMe groups in the ortho positions, which splits the n–π* transition into two absorption bands. The two isomeric forms can be obtained with more than 80 % enrichment from the respective photostationary state.

- Electrophilic alkynylation: the dark side of acetylene chemistry
  Brand, J. P.; Waser, J. *Chem. Soc. Rev.* **2012**, *41*, 4165-4179.
  Abstract:

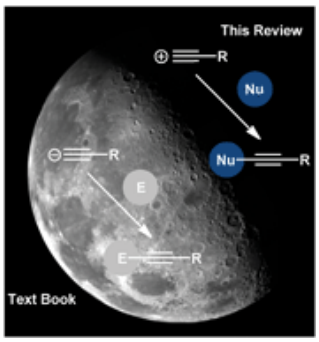

In addition to the well-established nucleophilic alkynylation, the use of electrophilic alkynes can expand tremendously the scope of acetylene transfer reactions. The use of metal catalysis has recently led to a rebirth of this research area. Halogenoalkynes, hypervalent alkynyliodoniums, acetylene sulfones and *in situ* oxidized terminal acetylenes are the most often used reagents for electrophilic alkynylation. Heteroatoms such as N, O, S and P can be now efficiently alkynylated. For

C–C bond formation, electrophilic acetylenes can be coupled with different organometallic reagents. Recently, the first breakthrough in direct C–H and C=C bond alkynylation has also been reported. Finally, sulfonyl acetylenes are efficient for alkyne transfer on carbon-centered radicals.

- Cyborg cells: functionalisation of living cells with polymers and nanomaterials
  Fakhrullin, R. F.; Zamaleeva, A. I.; Minullina, R. T.; Konnova, S. A.; Paunov, V. N. *Chem. Soc. Rev.* **2012**, *41*, 4189-4206.
  Abstract:

Living cells interfaced with a range of polyelectrolyte coatings, magnetic and noble metal nanoparticles, hard mineral shells and other complex nanomaterials can perform functions often completely different from their original specialisation. Such “cyborg cells” are already finding a range of novel applications in areas like whole cell biosensors, bioelectronics, toxicity microscreening, tissue engineering, cell implant protection and bioanalytical chemistry. In this tutorial review, we describe the development of novel methods for functionalisation of cells with polymers and nanoparticles and comment on future advances in this technology in the light of other literature approaches. We review recent studies on the cell viability and function upon direct deposition of nanoparticles, coating with polyelectrolytes, polymer assisted assembly of nanomaterials and hard shells on the cell surface. The cell toxicity issues are considered for many practical applications in terms of possible adverse effects of the deposited polymers, polyelectrolytes and nanoparticles on the cell surface.

- Dewetting-driven hierarchical self-assembly of small semiconducting molecules
  Tisserant, J. N.; Hany, R.; Partel, S.; Bona, G.; Mezzenga, R.; Heier, J. *Soft Matter* **2012**, *8*, 5804-5810.
  Abstract:

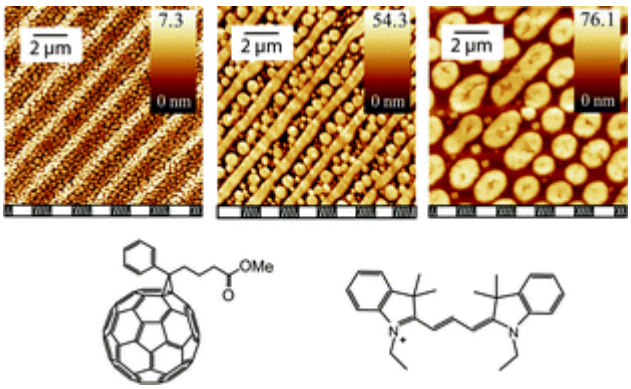

We describe the self-organization of PCBM and a cyanine dye on chemically patterned surfaces during spin coating from solution. On homogeneous surfaces, a transient bilayer forms, which in a later stage decomposes into PCBM droplets in a matrix of the cyanine dye. On the patterned surface

also a PCBM droplet phase develops, but the final film structure is greatly determined by contact line pinning of the PCBM domains to the substrate pattern. Three characteristic morphology regimes separated by wetting transitions were observed for different ratios between the natural domain dimensions and the underlying pattern periodicity. We demonstrate that contact line pinning can be an important means to control the film morphology in systems where films are coated from solution. This process can be exploited as a general and versatile method for patterning small semiconducting molecules into 1D and 2D photonic crystals.

- Solution-processed superhydrophobic conjugated polymer films
  Nyström, D.; Antoni, P.; Holdcroft, S.; Hult, A.; Malmström Jonsson, E.; Vamvounis, G. *Soft Matter* **2012**, *8*, 5753-5755.
  Abstract:

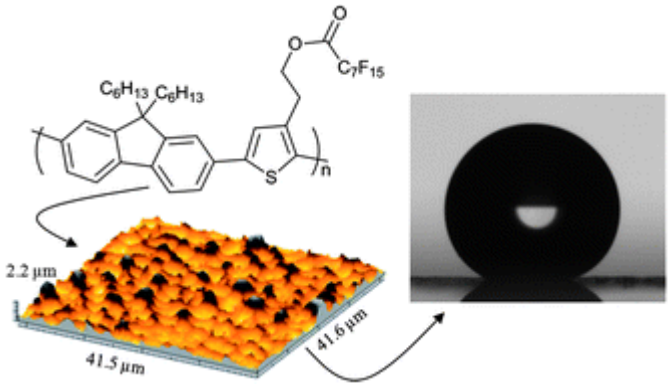

The interfacial properties of solution-processed conjugated polymer films are investigated. Their surface roughness was controlled by varying the humidity during the film deposition and mechanical exfoliation. A superhydrophobic film was obtained from a rough film of a partially fluorinated conjugated polymer. These films would be beneficial towards robust organic electronic devices.

- Charged nanoparticles as supramolecular surfactants for controlling the growth and stability of microcrystals
  Kowalczyk, B.; Bishop, K. J. M.; Lagzi, I.; Wang, D.; Wei, Y.; Han, S.; Grzybowski, B. A. *Nature Materials* **2012**, *11*, 227–232.
  Abstract:

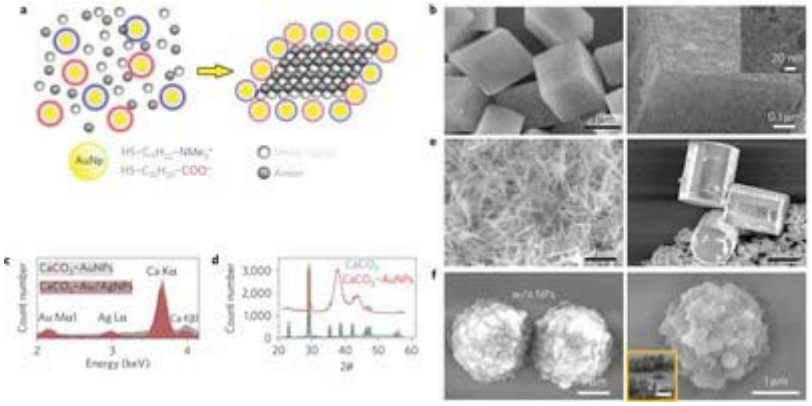

Microcrystals of desired sizes are important in a range of processes and materials, including controlled drug release, production of pharmaceutics and food, bio- and photocatalysis, thin-film solar cells and antibacterial fabrics. The growth of microcrystals can be controlled by a variety of agents, such as multivalent ions, charged small molecules, mixed cationic–anionic surfactants,

polyelectrolytes and other polymers, micropatterned self-assembled monolayers, proteins and also biological organisms during biomineralization. However, the chief limitation of current approaches is that the growth-modifying agents are typically specific to the crystalizing material. Here, we show that oppositely charged nanoparticles can function as universal surfactants that control the growth and stability of microcrystals of monovalent or multivalent inorganic salts, and of charged organic molecules. We also show that the solubility of the microcrystals can be further tuned by varying the thickness of the nanoparticle surfactant layers and by reinforcing these layers with dithiol crosslinks.

- Structure-guided evolution of cyan fluorescent proteins towards a quantum yield of 93%
  Goedhart, J.; Stetten, D.; Noirclerc-Savoye, M.; Lelimousin, M.; Joosen, L.; Hink, M. A.; Weeren, L.; Gadella, T. W. J.; Royant, A. *Nature Communications* **2012,** *3*, Article number: 751.
  Abstract:

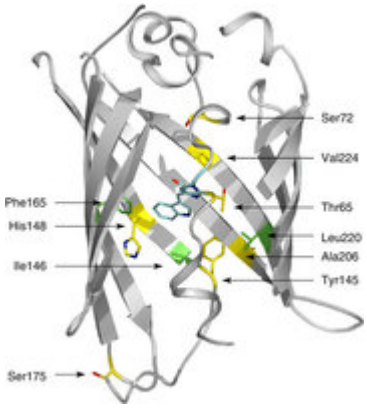

Cyan variants of green fluorescent protein are widely used as donors in Förster resonance energy transfer experiments. The popular, but modestly bright, Enhanced Cyan Fluorescent Protein (ECFP) was sequentially improved into the brighter variants Super Cyan Fluorescent Protein 3A (SCFP3A) and mTurquoise, the latter exhibiting a high-fluorescence quantum yield and a long mono-exponential fluorescence lifetime. Here we combine X-ray crystallography and excited-state calculations to rationalize these stepwise improvements. The enhancement originates from stabilization of the seventh β-strand and the strengthening of the sole chromophore-stabilizing hydrogen bond. The structural analysis highlighted one suboptimal internal residue, which was subjected to saturation mutagenesis combined with fluorescence lifetime-based screening. This resulted in mTurquoise2, a brighter variant with faster maturation, high photostability, longer mono-exponential lifetime and the highest quantum yield measured for a monomeric fluorescent protein. Together, these properties make mTurquoise2 the preferable cyan variant of green fluorescent protein for long-term imaging and as donor for Förster resonance energy transfer to a yellow fluorescent protein.